Acta of Bioengineering and Biomechanics
Vol. 18, No. 2, 2016

Original paper
DOI: 10.5277/ABB-00386-2015-02

The thumb carpometacarpal joint: curvature morphology of the articulating surfaces, mathematical description and mechanical functioning

HENNING DATHE[1], CLEMENS DUMONT[2], RAINER PERPLIES[1], JOCHEN FANGHÄNEL[3], DIETMAR KUBEIN-MEESENBURG[1], HANS NÄGERL[1], MARTIN M. WACHOWSKI[1, 4]*

[1] Biomechanical Working Group, Department of Orthodontics, University of Göttingen, Germany.
[2] Department of Trauma and Orthopaedic Surgery, Klinikum Kassel, Germany.
[3] Polyclinic of Orthodontics, University of Regensburg, Germany.
[4] Department of Trauma, Orthopaedics and Plastic Surgery, University of Göttingen.

Purpose: The purpose is to present a mathematical model of the function of the thumb carpometacarpal joint (TCMCJ) based on measurements of human joints. In the TCMCJ both articulating surfaces are saddle-shaped. The aim was to geometrically survey the shapes of the articulating surfaces using precise replicas of 28 TCMCJs. *Methods*: None of these 56 articulating surfaces did mathematically extend the differential geometrical neighbourhood around the main saddle point so that each surface could be characterised by three main parameters: the two extreme radii of curvature in the main saddle point and the angle between the saddles' asymptotics (straight lines). *Results*: The articulating surfaces, when contacting at the respective main saddle points, are incongruent. Hence, the TCMCJ has functionally five kinematical degrees of freedom (DOF); two DOF belong to flexion/extension, two to ab-/adduction. These four DOF are controlled by the muscular apparatus. The fifth DOF, axial rotation, cannot be adjusted but stabilized by the muscular apparatus so that physiologically under compressive load axial rotation does not exceed an angle of approximately ±3°. *Conclusions*: The TCMCJ can be stimulated by the muscular apparatus to circumduct. The mechanisms are traced back to the curvature incongruity of the saddle surfaces. Hence we mathematically proved that none of the individual saddle surfaces can be described by a quadratic saddle surface as is often assumed in literature. We derived an algebraic formula with which the articulating surfaces in the TCMCJ can be quantitatively described. This formula can be used to shape the articulating surfaces in physiologically equivalent TCMCJ-prostheses.

Key words: *thumb, saddle surfaces, curvature morphology, quantitative description, thumb kinematics*

1. Introduction

Both cartilaginous articulating surfaces of the thumb carpometacarpal joint (TCMCJ) are saddle-shaped. Under compressive joint loads this unique shape is said to allow only small contact areas. Hence, the large prevalence of osteoarthritis (AO) at the TCMCJ is attributed to high contact pressures loading the cartilage [3], [12], [13], [20], [28].

The articulating surfaces interact so that in ab-/adduction the concave part of the trapezium articulates with the respectively convex-shaped part of the os metacarpale, and that in flexion/extension the convex part of the trapezium now articulates with the respectively concave-shaped part of the os metacarpale [7], [15], [16], [22], [27], [30]. At the sides of ab- and adduction joint spaces were found to be partly filled with synovial foldings [22], [27]. In flexion/extension the articulating surfaces were said to be congruent [27].

Ateshian et al. [2] have surveyed both articulating surfaces by stereophotogrammetry (SPG) fitting each surface using a single parametric biquintic function. The differences between the two functions suggested a common curvature incongruence of the articulating

* Corresponding author: Martin M. Wachowski, Department of Trauma, Orthopaedics and Plastic Surgery, University of Göttingen, Robert-Koch-Str. 40, 37075 Göttingen, Germany. Tel: +49551396114, e-mail: martin.wachowski@web.de
Received: May 26th, 2015
Accepted for publication: July 6th, 2015

surfaces. Schmidt and Geissler [30] investigated both surfaces via silicon replicas. Cutting both replicas in a radio-ulnar or dorso-palmar direction, they confirmed common curvature incongruence. However, neither Schmidt and Geissler [30] nor Ateshian et al. [2] took the main saddle-point of the respective articulating surface into account, albeit at this unique point, the pair of the local main curvatures shows the *maximal* extreme values. At all other surface points the local extreme curvatures are smaller.

Our group developed a functional model of the TCMCJ [10] in which the joint's natural home position is given when the two articulating surfaces contact at the main saddle points of both articulating surfaces. By means of this functional model we qualitatively deduced some kinematical characteristics. In this study, we present the experimental confirmation of this model. For this purpose we at first remember the role of the main saddle point O (Fig. 1). At point O the saddle surface can be sectioned by two perpendicular planes, such that the cutting edge of both planes coincides with the normal in O, and the line of intersection, $k(z, x)$, is extremely concave, while the other, $k(y, z)$, is extremely convex. At all other points, the respective extreme curvatures are smaller than those at point O. To describe the saddle surface, the main point O is taken as the origin of the co-ordinate system, the normal in O as the z-axis, and the directions of the extreme curvatures as the y- or x-axis. Other planes that run through O and the z-axis produce intersecting lines whose curvature values at O are between the curvature values of $k(z, x)$ and $k(y, z)$. Because $k(z, x)$ is the extreme convex (positive curvature) and $k(y, z)$ is the extreme concave (negative curvature), two straight lines (curvature = 0), the so-called asymptotics, must exist among the intersection lines. These asymptotics are easily located by applying a straightedge at point O. In addition to the radii of curvature of the extreme contours the angle between the asymptotics, α, is the third crucial geometric parameter needed to characterise a saddle surface.

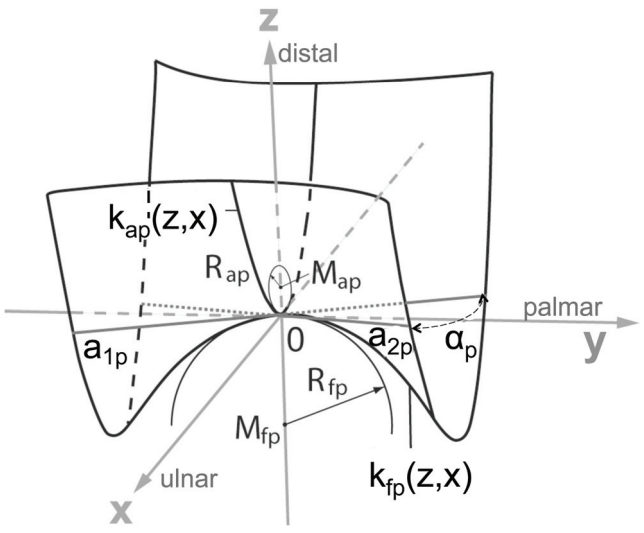

Fig. 1. Qualitative illustration of the saddle surface of the Os trapezium, it is the proximal articulating surface in the TCMCJ in lateral projection (left side). O = main saddle point. The extreme convex contour $k_{fp}(y, z)$ is practically aligned in flexion/extension, the extreme concave contour $k_{ap}(z, x)$ in ab/adduction. z-axis is directed to distal, y-axis to palmar, x-axis to ulnar. At the point O the contour $k_{fp}(y, z)$ has the curvature radius R_{fp} and contour $k_{ap}(z, x)$ the radius R_{ap}. The asymptotics through the main saddle point are a_{1p} and a_{2p}. They include the angle α_p

The purpose of this study is to present a mathematical model of the function of the TCMCJ based on the measurement of human joints.

Aims of the investigations in detail

1. To measure the radii of curvature of the extreme concave and convex contours as well as the angle between the asymptotics at the main saddle point for each articulating surface in order to describe quantitatively basic biomechanical properties of TCMCJ investigated.
2. To show empirically that each saddle surface represented the differential-geometrical neighbourhood around its main saddle point and to quantitatively describe the surface using a simple algebraic relation of the three measured parameters, both extreme radii of curvature and the angle between the asymptotics.
3. To discuss kinematical properties of the TCMCJ when the articulating surfaces contact at the main saddle points (home position).

Gender and body side were used as statistical variables.

2. Materials and methods

Data were collected from human autopsy material (Anatomic Institute, University of Greifswald). The specimens were preserved in a solution that largely maintains the stiffness and hardness of articular and osseous structures [14]. Altogether 28 TCMCJs were investigated from 7 females and 7 males aged 53–91 yrs (median of 81 yrs). The joints showed no signs of arthrosis.

At first we produced several accurate-scale replicas of the 56 articulating surfaces using highly precise dental moulding methods. We already successfully used this procedure to study the curvature morphology

of the articulating surfaces in interphalangeal and metacarpophalangeal joints in previous works [8], [9], [11]. On the accurate-scale models of the articulating surfaces we firstly scrutinized and marked the location of the main saddle point and the directions of the extreme curvatures using a straightedge and a binocular loupe. These models were sectioned through the main saddle point O along the extreme curvature contours $k(z, x)$ and $k(y, z)$ to produce the respective contours of ab-/adduction or flexion/extension. We precisely took into account that both planes must be perpendicular to each other. The main radii of curvature were determined by radii templates and the two asymptotics were determined using a straightedge on the replicas. The angle between the straight lines was measured using a simple angle gauge.

3. Results

In all 28 joints, each contour of extreme radii of curvature could be fitted within the functional range by a *circle*. Therefore each articulating surface was proven to be restricted to the mathematical neighbourhood around its main saddle point. Table 1 presents the radii of curvature and the angles between the asymptotics at the main saddle point. Table 2 presents the mean, standard deviation, *t*-, and *p*-values of the differences between the proximally and distally measured values. The centres of the extreme curvatures of the proximal surface were always located distal to the respective centres of curvature of the distal articulating surface; hence the differences in radii were always positive. On both articulating surfaces, the asymptotics intersected at almost 90 deg. Nevertheless, a small but statistically highly significant difference (3.5 deg) was observed between the angles of the proximal and distal asymptotics. Figure 2 illustrates these mean morphological parameters true to scale.

Table 1. Radii of the extreme curvatures and angles between the asymptotics at the main saddle point. The radii, whose centres of curvature were located distal/proximal from the articulating surface, were geometrically set positive/negative. This definition corresponds to the co-ordinate system in Fig. 1. The angles (α_p, α_d) were measured in the sector which included the contour line of flexion/extension. R_{ap}, R_{ad} = curvature radii in ab/adduction: R_{fp}, R_{fd} = curvature radii in flexion/extension

	Variable	Mean	SD	min	max
Proximal articulating surface	R_{ap}/mm	13.3	1.6	10.0	17.0
	R_{fp}/mm	–7.3	1.5	–5.0	–10.0
	α_p/deg	86.6	3.1	82.0	98.0
Distal articulating surface	R_{ad}/mm	11.0	1.2	9.0	13.0
	R_{fd}/mm	–8.1	1.2	–6.0	–10.0
	α_d/deg	90.1	2.5	86.0	96.0

Table 2. Difference statistics: In ab/adduction as well as in flexion/extension the differences between the radii of the extreme curvatures, measured at the main saddle point in each articulating surface, were highly significant. The angle between the asymptotics on the saddle surface of the Os trapezium was smaller than the respective angle on the saddle surface of the Os metacarpale I though both angles were near to 90 deg

Variable	Mean	SD	*t*-value	*p*
$(R_{ap} - R_{ad})$/mm	2.36	1.37	9.13	< 0.0001
$(R_{fp} - R_{fd})$/mm	0.82	1.12	3.87	< 0.0001
$(\alpha_p - \alpha_d)$/deg	–3.5	2.7	6.72	< 0.0001

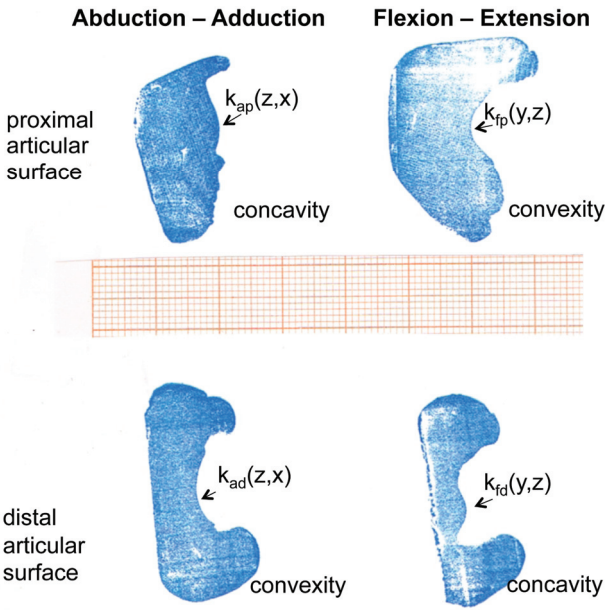

Fig. 2. Imprints of the four contours with extreme curvatures through the main saddle point of a TCMCJ (source document). The imprints were enlarged in order to read the respective radii of curvature by means of circular templates. The magnification factor was controlled by the scale paper. The main point O of the contours was found by comparison with the plaster casts and the original articular surfaces. Note: the contours have good picture sharpness

Detailed variance analyses (ANOVA) revealed that gender or body side were statistically insignificant.

Mathematical description of the articulating surfaces

If section planes did not include the normal in the main saddle point O, the section contours could have

unpredictable shapes; they could even be s-shaped, as Schmidt and Geissler [30] observed. By sectioning with two planes that meet at the curves $k(z, x)$ and $k(y, z)$ of the extreme curvatures, the inherent co-ordinate system of both saddle surfaces was found empirically. The plane curves $k(z, x)$ and $k(y, z)$ with the extreme curvatures defined the z-x- and the y-z-plane (Fig. 1). The cutting edge of both planes defined the normal (z-axis) in the main saddle point O, the origin of the coordinate system. Only by this procedure could mathematically interpretable data be obtained.

Since we did not observe any difference between the contours of the extreme curvatures at saddle point O and the approximating circles in any of the 4 times 28 individual sections (Fig. 2) it follows mathematically from these striking approximations that each articulating surface investigated can be generated by a set of plane parabolas whose apices coincide with main saddle point O and whose planes, which include the angle φ in the y-x-plane, run through the normal at point O. Curvature κ (= 1/R, R = curvature radius) in the apex defines every parabola definitely and κ solely depends on the angle φ

$$\kappa(\varphi) = 1/R(\varphi). \tag{1}$$

For quadratic saddle surfaces Euler wrote formula (1) to

$$\kappa(\varphi) = \kappa_f \cos^2\varphi + \kappa_a \sin^2\varphi\,. \tag{2}$$

Because the main curvatures κ_f and κ_a have opposite signs, there are two directions, $\varphi_\pm$, with vanishing curvature (asymptotic directions) which are determined by

$$0 = \kappa_f \cos^2\varphi_\pm + \kappa_a \sin^2\varphi_\pm\,. \tag{3}$$

It follows that

$$\tan^2\varphi_\pm = \frac{\sin^2\varphi_\pm}{\cos^2\varphi_\pm} = -\frac{\kappa_f}{\kappa_a} = \frac{R_a}{R_f}$$

$$\text{or} \quad \tan\varphi_\pm = \pm\sqrt{\frac{R_a}{R_f}}\,. \tag{4}$$

The angle α between the asymptotics is then given by

$$\alpha = \varphi_+ - \varphi_- = 2\arctan\sqrt{\frac{R_a}{R_f}}\,. \tag{5}$$

For quadratic saddle surfaces, the three parameters, which we have independently measured, the angle between the asymptotics (α), the radius of curvature in ad-/abduction (R_a), and the radius of curvature in flexion-/extension (R_f,) are definitely related.

Considering α = 90 deg, as approximately found for both surfaces (Table 1), it follows that R_a/R_f = 1. For each articulating surface, however, the ratio of the two extreme radii of curvature was much larger than 1 (proximal surface: R_{ap}/R_{fp} = 13.3/7.3 = 1.82; distal surface: R_{ad}/R_{fd} = 11.0/8.1 = 1.36; Table 1). Hence, the data proved that the TCMCJ saddles are definitively non-quadratic surfaces. The assumptions of Bausenhardt [4], Littler [24] and Marzke et al. [25] to model the articulating surfaces by quadratic hyperbolic surfaces are rejected and not applicable to the TCMCJ.

To derive an algebraic formula, which relates the curvature ($\kappa(\varphi)$) of the intersecting line for each intersection alignment (angle φ), we have to extend Euler's formula for quadratic saddle surfaces to non-quadratic surfaces in order to describe the TCMCJ [6].

First, we rewrite Euler's formula (2) as

$$\kappa(\varphi) = \kappa_f \cos^2\varphi + \kappa_a \sin^2\varphi = \kappa_f \frac{1}{2}(1+\cos 2\varphi)$$

$$+ \kappa_a \frac{1}{2}(1-\cos 2\varphi) = \frac{1}{2}(\kappa_f + \kappa_a) + \frac{1}{2}(\kappa_a - \kappa_f)\cos 2\varphi$$

or

$$\kappa(\varphi) = c_0 + c_2 \cos 2\varphi\,. \tag{6}$$

We interpret this Euler equation (6) as a Fourier series truncated after the second harmonic – and we propose truncating the Fourier series after the fourth harmonic

$$\kappa(\varphi) = c_0 + c_2 \cos 2\varphi + c_4 \cos 4\varphi\,. \tag{7}$$

Equation (7) has an additional constant to describe the curvature as function of angle φ. Inserting three measured curvatures into equation (7) leads to a solvable system of equations for the constants c_0, c_2 and c_4.

With the mean values measured on the proximal surface (κ_{fp} = 1/R_{fp} = 1/7.3 mm; κ_{ap} = 1/R_{ap} = –1/13.3 mm; α = 86.6 deg) the mean proximal surface is given by

$$\kappa_p(\varphi) = 1/R_p = 0.0122\ \text{mm}^{-1} + 0.106\ \text{mm}^{-1}\cdot\cos(2\varphi)$$

$$+ 0.0187\ \text{mm}^{-1}\cdot\cos(4\varphi), \tag{7a}$$

and quantitatively illustrated in Fig. 3.

Consequently, the simplest mathematical procedure is to generate each articulating surface by parabolas, whose symmetry axes coincide with the z-axis, whose apices coincide with the main saddle point O, and whose main curvature in the apices depends on the rotational

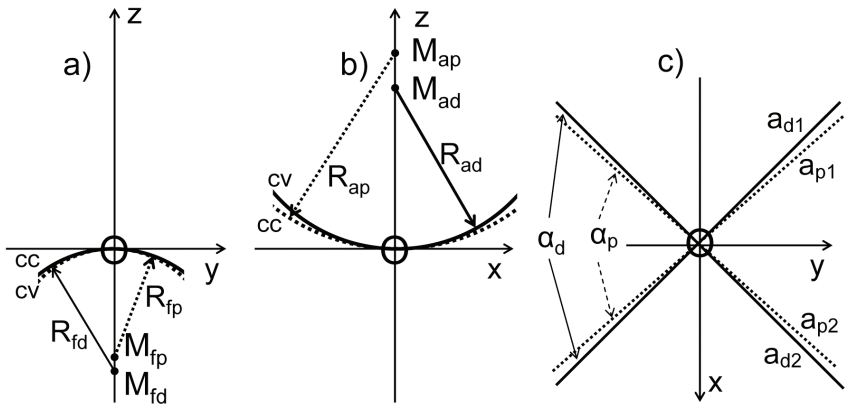

Fig. 3. Contours of intersections through the TCMCJ in home position, true to scale corresponding to Table 1:
The two articulating surfaces contact in the respective main saddle points.
By that the common origin O of the co-ordinate systems is defined.
Full/pointed lines: Contours of the distal/proximal articulating surface. cv = convex, cc = concave contours.
(a) The *y*-*z*-plane cuts the articulating surfaces in flexion/extension producing contours of extreme curvatures.
The concave contour (cc) of the distal surface has the larger radius of curvature ($R_{fd} > R_{ad}$).
The respective centre of curvature M_{fd} is proximally located from the centre of curvature M_{fp} of the proximal articulating surface;
(b) The *x*-*z*-plane cuts the articulating surfaces in ab/adduction producing also the contours of extreme curvatures.
The centre of curvature M_{ap} of the concave contour of the proximal articulating surface (radius R_{ap})
is distally positioned to the centre of curvature M_{ad} of the convex contour of the distal articulating surface (radius R_{ad});
(c) The *y*-*x*-plane cuts the distal saddle surface in asymptotics a_{d1} and a_{d2} showing angle α_d
and the proximal saddle surface in asymptotics a_{p1} and a_{p2} (angle α_p)

angle φ around the *z*-axis. The functional range of the articulating surfaces, in all TCMCJs investigated, was found to be limited to the mathematical region near the main saddle point. In this region, each parabola can be approximated by the radius of curvature of its apex. In Fig. 3, the illustration of the saddle surface exceeds this mathematical neighbourhood. The functional part of the surface lies within 7 mm of the main saddle point as is made evident by the functional cuts (Fig. 2). In contrast to Ateshian et al. [1], both articulating surfaces are described by rather simple algebraic relations with only one independent variable (angle φ).

Furthermore, formula (7) gives the essential key for shaping the articulating surfaces of functional TCMCJ endoprostheses.

4. Discussion

4.1. Curvature incongruence of the articulating surfaces

Regarding the TCMCJ, Du Bois-Reymond [7] wrote: "The radii of the curvatures of the articulating surfaces, which belong together, are considerably different. A stronger convex curvature always touches a weaker concave curvature." As mentioned above, Ateshian et al. [1] and Schmidt and Geissler [30] referred to this curvature incongruence. Our measurements confirmed these statements quantitatively; significant differences in radii were up to 11% in flexion/extension and 21% in ab/adduction. At the home position, the joint has only one contact point, which enlarges under a compressive force to a small contact area according to the law of Hertz [23].

4.2. Number of kinematical degrees of freedom of the TCMCJ

For more than 150 years, the prevalent doctrine in functional anatomy has assumed that the TCMCJ has only two kinematical degrees of freedom (DOF), i.e., that only one stationary rotational axis for flexion/extension and one for ab-/adduction would exist [2], [5], [15]–[17], [19], [20]. Hollister et al. [18] tried to determine these two assumed axes using a method similar to axiography of the temporomandibular joint in dentistry. Nägerl et al. [26] have shown that axiography determines the position of a non-stationary instantaneous rotational axis (IRA) given by two independent instantaneous rotations around a mandibularly and a maxillarily fixed axis. Hence, Hollister did not determine the number of DOF in the TCMCJ.

In guiding joint motions, the two incongruent articulating surfaces have biomechanically equal rights [8], [10]. Hence, out of home position, TCMCJ-flexion/extension can be performed by rotations around the curvature centres M_{fd} and M_{fp} or simultaneously around both (Fig. 4). Similarly ab-/adduction can also occur by independent rotations around two centres (M_{ad} and/or M_{ap}, Fig. 4). Because the angles between the asymptotics differ for the saddle surfaces, a small axial rotation can occur when first moving out of home position. During this small rotation the contact at the saddle points remains constant (Fig. 4). Hence, our measurements proved that the TCMCJ has five kinematical DOFs according to five morphologically given axes as previously suggested [10] by our group. Analogously we found five DOFs for the metacarpophalangeal joint [11], which is usually said to be a "ball-and-socket" joint with three DOFs. In both joints, the four DOF of ab-/adduction and flexion/extension are actively controlled by the muscular apparatus. Axial rotation, however, can only passively follow an external axial torque.

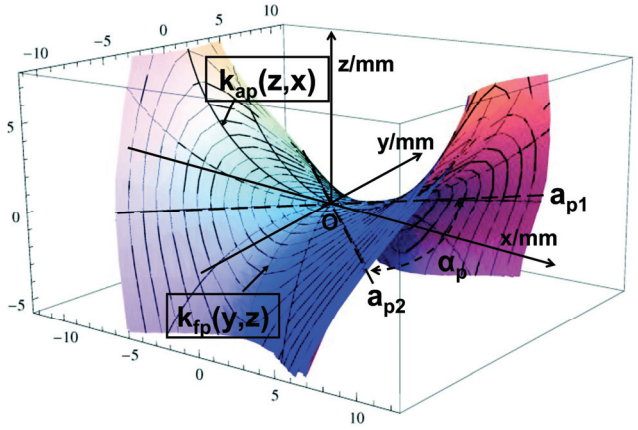

Fig. 4. Type of non-quadratic saddle surfaces of the thumb TCMCJ. The illustration shows the mean proximal surface true to scale. The surface is generated by parabolas. The apices of the parabolas $k_{ap}(z, x)$ and $k_{fp}(y, z)$ have the extreme curvatures $\kappa_{ap}(z, x)$ and $\kappa_{fp}(y, z)$. The asymptotics (a_{p1}, a_{p2}) have vanishing curvature. Point O, the origin of the co-ordinate system, is the common apex of all intersecting parabolas. The surface drawn exceeds the area of the biological articulating surface which is mathematically limited to the differential geometric neighbourhood around the main saddle point O which hardly exceeds the radius of 10 mm around point O

4.3. Stabilisation of axial rotation in TCMCJ

Because both the TCMCJ and MCPJ have five DOF, the question of the mechanical advantage of the saddle shape arises. In the MCPJ, the egg-shaped proximal joint surface articulates in a wider cup, and axial rotations are hindered only by ligaments [29]. In the TCMCJ, however, there is a unique mechanism of axial stabilisation as we previously suggested [11]: After axial rotations of ≈ ±1.75 deg, the asymptotics of the proximal and distal surface coincide such that the contact "point" is enlarged to a contact "line". As soon as the rotational angle exceeds 1.75 deg, the contact "line" splits into two contact "points". These contact points are located at outer areas of the articulating surfaces, causing a dehiscence to emerge in the centre of the TCMCJ. Subsequently, the trapezium and the metacarpal bone spiral apart, as was already observed by Du Bois-Reymond [7] and demonstrated by Köbke and Thomas [21] in experiments on models. Indeed, the muscular apparatus acting on the TCMCJ is then not able to produce axial rotation, but it can produce high resulting compressive force. This muscular force is compensated by two joint forces, whose lines run through the contacts and do not intersect because of the special shape of the saddle. Therefore, a resulting counteracting torque is produced, which directly increases with dehiscence size when further axial rotation occurs. This torque hinders further axial rotation and/or spirals the joint back to home position. Thus, in the TCMCJ, axial rotation is essentially stabilised by the muscular apparatus in a simple way; the muscles need only to produce a compressive resultant force. In the MCPJ this mechanism fails because the shapes of the articulating surfaces do not allow two temporary contacts. This stabilisation of axial rotation corresponds to the report by Cooney and Chao [5] stating that under loads axial rotation in the TCMCJ is always small.

4.4. Rolling of the articulating surfaces in the TCMCJ and circumduction

Napier [27] and Kuczynski [22] illustrated that, during ab/adduction, the contact area simultaneously migrated on *both* articulating surfaces in the same direction, causing the joint space to open behind. Ateshian et al. [2] confirmed these findings of Napier and Kuczynski and additionally described an analogous migration of the contact area during flexion/extension. The contact area was shifted towards volar regions not only on the trapezium but simultaneously also on the metacarpal. The findings of Napier, Kuczynski, and Ateshian demonstrate that the articulating surfaces roll to a certain extent during ab-/adduction or flexion/extension. In the MCPJ, partially

rolling cannot occur because the contact area migrates on the articulating surfaces in opposite directions during flexion/extension and ab-/adduction [10].

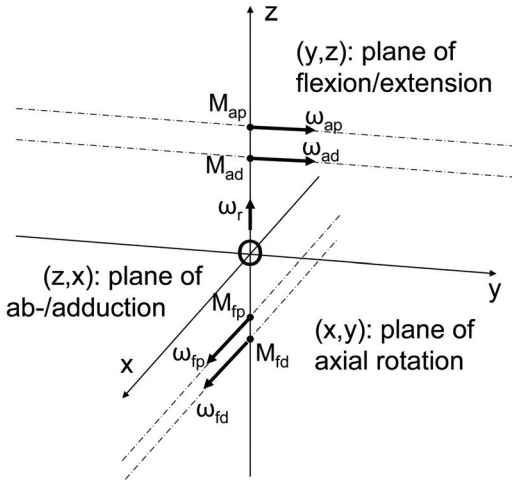

Fig. 5. Kinematical functions and geometrical alignment of the five kinematical DOFs of the TCMCJ in home position (according to [15]): the angular velocities ω_{ap} and ω_{ad} around the morphologically given axes M_{ap} and M_{ad} in ab/adduction are perpendicular to the angular velocities ω_{fp} and ω_{fd} around the morphologically given axes M_{fp} and M_{fd} in flexion/extension. The position of the axes are given by the radii of curvature measured in the saddle point: $OM_{ap} = R_{ap}$, $O_{ad} = R_{ad}$, $OM_{fp} = R_{fp}$, $OM_{fd} = R_{fd}$ (Table 1). ω_r = angular velocity of axial rotation

When considering pure rolling (Fig. 5) the instantaneous rotational axis must run through the contact. According to the laws of kinematics, this would take place if the neuromuscular apparatus met the following conditions on the angular velocities:

Ab-/adduction:

$$\vec{\omega}_a = \vec{\omega}_{ap} + \vec{\omega}_{ad}\,, \quad \text{with} \quad -\frac{\omega_{ap}}{\omega_{ad}} = \frac{R_{ad}}{R_{ap}}\,. \tag{8}$$

Flexion/extension:

$$\vec{\omega}_f = \vec{\omega}_{fp} + \vec{\omega}_{fd}\,, \quad \text{with} \quad -\frac{\omega_{fp}}{\omega_{fd}} = \frac{R_{fd}}{R_{fp}}\,. \tag{9}$$

Rolling circumduction: In general, it is possible to guide the extended thumb around a cone, whose apex lies in the TCMCJ. Therefore, the metacarpal bone does not axially rotate. In this case, the motions of ab-/adduction and flexion/extension must be phase-delayed.

$$\vec{\omega}_{res} = \vec{\omega}_a + \vec{\omega}_f \quad \text{with} \quad \vec{\omega}_a = \vec{\omega}_{ao} \cdot \cos(\Omega t)$$
$$\text{and} \quad \vec{\omega}_f = \vec{\omega}_{fo} \cdot \sin(\Omega t)\,. \tag{10}$$

When the angular velocities ($\vec{\omega}_a$ and $\vec{\omega}_f$) alternate according to equations (10), the resulting instantaneous axis of rotation, IRA_{res}, pivots about the z-axis of the proximal articulating surface. Correspondingly, the long axis of the metacarpal bone moves along a cone-shaped shell without rotating around its long axis. The circumduction occurs in a rolling manner; the contact of the articulating surfaces circulates around the z-axis of the CMCJ in conjunction with the respective joint space on the opposite side.

5. Conclusions

The articulating surfaces of the TCMCJ cannot be approximated by quadratic saddle surfaces, as is commonly thought. The data show that Euler's formula for quadratic saddles is not valid for the articulating surfaces of the os trapezium or os metacarpale I.

Each saddle surface can be quantitatively described by the extended Euler relation $\kappa(\varphi) = c_0 + c_2 \cdot \cos(2\varphi) + c_4 \cdot \cos(4\varphi)$ around its main point. The surfaces can be approximated by a set of parabolas whose curvatures, $\kappa(\varphi)$, in the apices follow the extended Euler relation.

The articulating surfaces of the TCMCJ show considerable curvature incongruence.

The TCMCJ has five kinematical DOFs. Flexion/extension and ab-/adduction have one DOF for each articulating surface such that flexion/extension and ab-/adduction have four total DOFs actively controlled by the muscular apparatus. The passive kinematical DOF of axial rotation is automatically stabilised by the muscular apparatus when producing a compressive joint force.

Circumduction can be controlled by the muscular apparatus in such a way that the articulating surfaces predominantly roll over one another. By that friction is reduced.

The presented data give clear outlines for the construction of a functional prosthesis for the TCMCJ.

References

[1] ATESHIAN G.A., ARK J.W., ROSENWASSER M.P., PAWLUK R.J., SOSLOWSKY L.J., MOW V.C., *Contact areas in the thumb carpometacarpal joint*, J. Orthop. Res., 1995, Vol. 13(3), 450–458.

[2] ATESHIAN G.A., ROSENWASSER M.P., MOW V.C., *Curvature characteristics and congruence of the thumb carpometacarpal joint: differences between female and male joints*, J. Biomech., 1992, Vol. 25(6), 591–607.

[3] AUNE S., *Osteo-arthritis in the first carpo-metacarpal joint; an investigation of 22 cases*, Acta Chir. Scand., 1955, Vol. 109(6), 449–456.

[4] BAUSENHARDT D., *Über das Carpometacarpalgelenk des Daumens*, Z. Anat. Entwickl.-Gesch., 1949, Vol. 114, 251.

[5] COONEY W.P. 3RD, CHAO E.Y., *Biomechanical analysis of static forces in the thumb during hand function*, J. Bone Joint Surg. Am., 1977, Vol. 59(1), 27–36.

[6] DATHE H., *Die Form von Gelenkflächen – Morphometrie mit einfachen Mitteln*, Universitätsverlag Göttingen, Göttingen, 2012.

[7] DU BOIS-REYMOND R., *Über das Sattelgelenk*, Arch. Anat. Physiol., 1985, 433–462.

[8] DUMONT C., ALBUS G., KUBEIN-MEESENBURG D., FANGHANEL J., STURMER K.M., NAGERL H., *Morphology of the interphalangeal joint surface and its functional relevance*, J. Hand Surg. Am., 2008, Vol. 33(1), 9–18.

[9] DUMONT C., BURFEIND H., KUBEIN-MEESENBURG D., HOSTEN N., FANGHANEL J., GREDES T., NAGERL H., *Physiological functions of the human finger*, J. Physiol. Pharmacol., 2008, Vol. 59, Suppl 5, 69–74.

[10] DUMONT C., PERPLIES R., DOERNER J., FANGHAENEL J., KUBEIN-MEESENBURG D., WACHOWSKI M.M., NAEGERL H., *Mechanisms of circumduction and axial rotation of the carpometacarpal joint of the thumb*, J. Physiol. Pharmacol., 2009, Vol. 60, Suppl 8, 65–68.

[11] DUMONT C., ZIEHN C., KUBEIN-MEESENBURG D., FANGHANEL J., STURMER K.M., NAGERL H., *Quantified contours of curvature in female index, middle, ring, and small metacarpophalangeal joints*, J. Hand Surg. Am., 2009, Vol. 34(2), 317–325.

[12] EATON R.G., GLICKEL S.Z., *Trapeziometacarpal osteoarthritis. Staging as a rationale for treatment*, Hand Clin., 1987, Vol. 3(4), 455–471.

[13] EATON R.G., LITTLER J.W., *Ligament reconstruction for the painful thumb carpometacarpal joint*, J. Bone Joint Surg. Am., 1973, Vol. 55(8), 1655–1666.

[14] FANGHÄNEL J., SCHULTZ F., *Mitteilung über eine Konservierungsflüssigkeit für anatomisches Präpariermaterial*, Zeitschrift für Medizinische Labortechnik, 1962, Vol. 3, 329–332.

[15] FICK A., *Die Gelenke mit sattelförmigen Flächen*, Z. rat. Med. (N.F.), 1854, Vol. 4, 314–321.

[16] FICK R., *Handbuch der Anatomie und Mechanik der Gelenke. Zweiter Teil: Allgemeine Gelenk- und Muskelmechanik*, Verlag von Gustav Fischer, Jena, 1910.

[17] FISCHER O., *Über Gelenke mit zwei Graden der Freiheit*, Arch. Anat. Physio. (Anat. Abt) 1897, Suppl., 242–272.

[18] HOLLISTER A., GIURINTANO D.J., BUFORD W.L., MYERS L.M., NOVICK A., *The axes of rotation of the thumb interphalangeal and metacarpophalangeal joints*, Clin. Orthop. Relat. Res., 1995, Vol. 320, 188–193.

[19] KAPANDJI I.A., *Funktionelle Anatomie der Gelenke.* Bd. 1: *Obere Extremität*, Ferdinand Enke Verlag Stuttgart, 1984, 218.

[20] KÖBKE J., *Funktionelle Anatomie des Daumensattelgelenks, Daumensattelgelenksarthrose*, D. Buck-Gramcko, B. Helbig (eds.), Hippokrates, Stuttgart, 1994, 13–19.

[21] KÖBKE J., THOMAS W., *Biomechanical investigations on the aetiology of arthrosis of the first carpometacarpal joint* (author's transl.). Z Orthop. Ihre Grenzgeb., 1979, Vol. 117(6), 988–994.

[22] KUCZYNSKI K., *Carpometacarpal joint of the human thumb*, J. Anat., 1974, Vol. 118(Pt 1), 119–126.

[23] LANDAU L.D., LIFSCHITZ E.M., *Elastizitätslehre*, Akademie-Verlag, Berlin, 1966.

[24] LITTLER J.W., *The architectural and functional principles of the anatomy of the hand*, Rev. Chir. Orthop. Reparatrice Appar. Mot., 1960, Vol. 46, 131–138.

[25] MARZKE M.W., TOCHERI M.W., MARZKE R.F., FEMIANI J.D., *Three-dimensional quantitative comparative analysis of trapezial-metacarpal joint surface curvatures in human populations*, J. Hand Surg. Am., 2012, Vol. 37(1), 72–76.

[26] NÄGERL H., KUBEIN-MEESENBURG D., SCHWESTKA-POLLY R., THIEME K.M., FANGHANEL J., MIEHE B., *Functional condition of the mandible: physical structures of free mandibular movement*, Ann. Anat., 1999, Vol. 181(1), 41–44.

[27] NAPIER J.R., *The form and function of the carpo-metacarpal joint of the thumb*, J. Anat., 1955, Vol. 89(3), 362–369.

[28] PELLEGRINI V.D. Jr., *Osteoarthritis of the trapeziometacarpal joint: the pathophysiology of articular cartilage degeneration. I. Anatomy and pathology of the aging joint*, J. Hand Surg. Am., 1991, Vol. 16(6), 967–974.

[29] RAUBER A., KOPSCH F., BAND I, *Bewegungsapparat. Anatomie des Menschen*, B. Tillmann, G. Töndury, K. Zilles (eds.), Thieme, Berlin 2003.

[30] SCHMIDT H.M., GEISSLER B., *Joint surfaces of the carpometacarpal articulation of the thumb in man*, Gegenbaurs Morphol. Jahrb., 1983, Vol. 129(5), 505–531.